Synthesis, structural, optical and anti-rheumatic activity of metal complexes derived from *(E)*-2-amino-N-(1-(2-aminophenyl)ethylidene)benzohydrazide (2-AAB) with Ru(III), Pd(II) and Zr(IV)

Nasser Mohammed Hosny, Yousery E. Sherif

PII: S1386-1425(14)01422-X
DOI: http://dx.doi.org/10.1016/j.saa.2014.09.064
Reference: SAA 12740

To appear in: *Spectrochimica Acta Part A: Molecular and Biomolecular Spectroscopy*

Received Date: 31 July 2014
Revised Date: 11 September 2014
Accepted Date: 18 September 2014

Please cite this article as: N.M. Hosny, Y.E. Sherif, Synthesis, structural, optical and anti-rheumatic activity of metal complexes derived from *(E)*-2-amino-N-(1-(2-aminophenyl)ethylidene)benzohydrazide (2-AAB) with Ru(III), Pd(II) and Zr(IV), *Spectrochimica Acta Part A: Molecular and Biomolecular Spectroscopy* (2014), doi: http://dx.doi.org/10.1016/j.saa.2014.09.064

Synthesis, structural, optical and anti-rheumatic activity of metal complexes derived from *(E)*-2-amino-N-(1-(2-aminophenyl)ethylidene)benzohydrazide (2-AAB) with Ru(III), Pd(II) and Zr(IV)

Nasser Mohammed Hosny [*1], Yousery E. Sherif[2,3]

[1]*Chemistry Department, Faculty of Science, Port-Said University, 23 December Street, Port-Said, Egypt*
[2]*Department of Chemistry, Faculty of Science and Arts, Ulla, Taibah University, KSA.*
[3]*Clinical Pharmacology Department, Faculty of Medicine, Mansoura University, Mansoura, Egypt*

ABSTRACT

Three new metal complexes derived from Pd(II), Ru(III) and Zr(IV) with *(E)*-2-amino-N-(1-(2-aminophenyl)ethylidene)benzohydrazide (2-AAB) have been synthesized. The isolated complexes were characterized by elemental analyses, FT-IR, UV-Vis., ES-MS, ^{1}HNMR, XRD, thermal analyses (TGA and DTA) and conductance. The morphology and the particle size were determined by transmittance electron microscope (TEM). The results showed that, the ligand coordinates to Pd(II) in the enol form, while it coordinates to Ru(III) and Zr(IV) in the keto form. A square planar geometry is suggested for Pd(II) complex and octahedral geometries are suggested for Ru(III) and Zr(IV) complexes. The optical band gaps of the isolated complexes were measured and indicated the semi-conductivity nature of the complexes.

The anti-inflammatory and analgesic activities of the ligand and its complexes showed that, Ru(III) complex has higher effect than the well known drug "meloxicam".

Keywords: Ru(III); Pd(II); Zr(IV); Metal complexes; Anti-inflammatory activity

---

[*]Corresponding author:
Tel.:00201208949300
E-mail: Nasserh56@yahoo.com

Introduction

Hydrazones are considered one of the most important classes of compounds from the inorganic and biological point of view. They have thermal, mechanical, electrical and magnetic properties. Also, hydrazones have non-linear optical and liquid-crystal properties [1-4]. These properties made them the subject of wide applications in analytical chemistry, in synthesizing novel heterogeneous catalysts in redox processes and in molecular semi-conductors [5]. Besides that, hydrazones and their coordination compounds have been investigated widely in medicine, especially as anti-tuberculosis, anti-tumor, anti-hypertensive and peripheral vasodilator agents [6-10]. Anti-inflammatory studies indicated that, hydrazones derivatives have lower side effects compare with the non-steroidal anti-inflammatory drugs (NSAIDs) [11-12].

In this work we synthesized new metal complexes of Pd(II), Ru(III) and Zr(IV) with *(E)*-2-amino-N-(1-(2-aminophenyl)ethylidene)benzohydrazide (2-AAB). The isolated complexes have been characterized by different techniques to elucidate the structure. To shed more light on the potential applications of the present compounds, the optical band gaps of the complexes have been measured. Also, the analgesic and anti-inflammatory activities of (2-AAB) and its metal complexes have been studied and compared with meloxicam.

Experimental

The chemicals used were of analytical grade and were used without further purification. Conductvity was carried out on YSI model 32 conductivity bridge. The metal ions were determined by standard methods [13]. The elemental analyses, C, H and N were carried out on Thermo Scientific Flash 2000 Analyzer. IR spectra were carried out on a Mattson 5000 FTIR spectrometer by using KBr discs. UV-visible spectra were taken by UV2 Unicam UV/vis spectrometer by using 1 cm silica cell. TGA and DTA were measured on a Shimadzu model 50 H device, the flow rate of nitrogen is 20 cm^3/min. and the heating is 10 ^oC/min. JEOL spectrophotometer (500 MHz) was

used to measure ^{1}H-NMR spectra by using TMS as reference and DMSO-d_6 as solvent. TEM images of the products were obtained by CM20PHILIPS electron microscope. XRD measurements were carried out on a D2PHASER Bruker diffractometer using CuKα radiation (λ = 1.540598 Å). The microcrystalline samples were ground in an agate mortar, and then deposited in silicon sample holder equipped with a zero-background plate. Diffraction data were collected in the 2θ range of 5-40°, with 0.02° steps.

Synthesis of (E)-2-Amino-N-(1-(2-aminophenyl)ethylidene)benzohydrazide (2-AAB)

0.02 mol (4.8 ml) of 2-aminoacetophenone was injected to 0.02 mol (3.0 gm) of 2-aminobenzohydrazide in 25 ml ethanol. The reaction was refluxed for 6 hrs. Yellow crystals were formed. The precipitate was filtered under vacuum then, washed with ethanol and kept under vacuum. % Yield 85, M Wt = 269.325; *Found,* Calcd. for $C_{15}H_{17}N_4O$: C, 66.3; H, 6.9; N, 21.0 Calcd: C, 66.8; H, 6.3; N, 20.8%. ^{1}H NMR (DMSO-d_6): δ/ppm 2.34 (s, 3H, CH_3-), 6.28 (s, 2H, NH_2-), 6.51 (s, 2H, NH_2-), 6.71-7.58 (m, 8H, C_6H_4) and 10.64 (s, 1H, NH-).

Synthesis of Zr (IV) complex

To 0.01 mol (2.86 gm) of *(E)*-2-amino-N-(1-(2-aminophenyl)ethylidene)benzohydrazide (2-AAB) in 25 ml ethanol, 0.01 mol (1.41 gm) of $ZrCl_4$ was injected and refluxed under nitrogen for 6 hrs. A yellow precipitate was isolated. The precipitate was filtered under vacuum then, washed with ethanol and kept under vacuum.

% Yield 74; M. Wt = 525.388*; Found,* Calcd. for $[Zr(C_{15}H_{17}N_4O)Cl_4]0.5EtOH$: C, 36.2; H, 3.4; N, 10.1; Zr, 16.8%. Calcd: C, 36.6; H, 3.8; N, 10.7; Zr, 17.3%. ^{1}H NMR (DMSO-d_6): δ/ppm 2.30 (s, 3H, CH_3-), 6.10 (s, 2H, NH_2-), 6.41 (s, 2H, NH_2-), 6.68-7.82 (m, 8H, C_6H_4) and 10.60 (s, 1H, NH-).

Synthesis of Pd(II) complex

0.01 mol (2.94 gm) of Na_2PdCl_4 in 10 ml distilled water was added to 0.01 mol (2.86 gm) of *(E)*-2-amino-N-(1-(2-aminophenyl)ethylidene)benzohydrazide (2-AAB) in 25 ml ethanol. The reaction was refluxed for 4 hrs. An orange precipitate was formed. The precipitate was filtered under vacuum and washed with ethanol and finally kept under vacuum.

% Yield 78; M. Wt = 539.77, *Anal.* Calc. for $[Pd(C_{15}H_{16}N_4O)Cl\ H_2O]2H_2O$: C, 38.8; H, 4.7; N, 12.1; Pd, 20.6%. Found: C, 39.2; H, 5.0; N, 12.5; Pd, 19.7 %. ^{1}H NMR (DMSO-d_6): δ/ppm 2.43 (s, 3H, CH_3-), 6.51 (s, 2H, NH_2-), 6.71 (s, 2H, NH_2-), 7.10-7.91 (m, 8H, C_6H_4).

Synthesis of Ru(III) complex

0.01 mol (2.6 gm) of $RuCl_3.3H_2O$ in 10 ml ethanol was added to 0.01 mol (2.86 gm) of *(E)*-2-amino-N-(1-(2-aminophenyl)ethylidene)benzohydrazide (2-AAB) in 25 ml ethanol. The reaction was refluxed for 4 hrs. A dark green precipitate was isolated. The precipitate was filtered under vacuum then, washed with ethanol and kept under vacuum.

% Yield 83; M Wt = 547.01. *Found.* Calcd. $[Ru(C_{15}H_{17}N_4O).3Cl.H_2O]2.5H_2O$: C, 32.8; H, 4.6; N, 9.7; Ru, 19.0%. Found: C, 33.2; H, 4.4; N, 10.3; Ru, 18.5%

Pharmacological studies

The anti-inflammatory was carried out by carrageenan induced rat hind paw edema method on Sprague-Dawley rats (200–250 g). The animals were divided into two main groups [arthritic group (n = 36) and control of non arthritic (n = 6)] [14,15]. Gastric tube once daily was used to give orally the tested compounds for seven days. Paget's table was used to calculate the dose [16]. The experiments and animal care were carried out according to NIH guide to the care and use of laboratory animals. The study was approved by the local ethical committee. The compounds were suspended in 0.5% sodium carboxymethyl cellulose [SCMC] mg per 200 g of rat weight because of the insolubility of the compounds. The analgesic activity of the tested compounds was determined by measuring right paw pad pressure tolerance at the 7th day of the compound administration (52 days after complete Freund's adjuvant injection). Analgesimeter (Ugo Basile, Italy) was used to apply pressure on the rat pad of the right paw.

Results and discussion

The isolated complexes are stable in air, colored, soluble in DMF and DMSO but insoluble in water and common organic solvents. The molar conductivity values of $1x10^{-3}$ molar in DMF at 25°C are in the range 5.0-10.0 $\Omega^{-1}cm^2mol^{-1}$. The conductivity values indicate non-conducting nature

of the compounds [17]. The ligand (2-AAB) can exist either in the keto form Fig. 1(A) or in the enol form Fig.1 (B). Some important IR bands are collected in Table 1.

The infrared spectrum of (2-AAB) shows bands at 3480, 3458, 3366 and 3215 cm^{-1} assigned to ν (NH_2) of the amino groups. The bands at 1631, 1612, 1600, 1574 and 970 cm^{-1} can be attributed to ν (C=O), δ (NH_2), ν (C=N), ν (CONH) and ν (N-N) modes, respectively [18-20]. The presence of the bands attributed to ν (C=O) and ν (CONH) confirms the existence of the free ligand in the keto form.

The spectra of Zr(IV) and Ru(III) complexes exhibit bands in the region 1645-1666 cm^{-1} attributed to ν (C=O). The shift of these bands compared with their positions in the free ligand, confirms the participation of this group in bonding. The presence of the band assigned to ν (CONH) in the spectra of these two complexes suggests that (2-AAB) chelates to these metal ions in the keto form (Figs. 2, 3 and 4). The disappearance of the bands assigned to ν (C=O) and ν (CONH) in the spectrum of Pd(II) complex together with the appearance of a new band at 1608 cm^{-1} assigned to ν $(C=N)^{*}$ indicates the enolization of the carbonyl group. The enolic carbonyl is deprotonated after coordination. The band suggested to the azomethine group ν (C=N) is shifted in all the metal complexes, indicating the participation of this group in bonding. Also, the shift to higher frequency of the band at 970 cm^{-1} assigned to ν (N-N) supports the participation of azomethine group as an active site. The new weak bands in the regions 440-489 and 530-570 cm^{-1} can be assigned to ν (M-N) and ν (M-O), respectively [21]. The appearance of weak bands in the regions 684-699 cm^{-1} and 744-786 cm^{-1} attributed to ρ_w (OH) and δ(OH), respectively confirms the presence of water or ethanol molecules in the complexes [22].

The ^{1}H-NMR spectrum of the ligand (Fig. 5), in DMSO-d_6 shows singlet signal at 10.64 ppm of -NH amidic protons. Another singlet signal is observed at 2.34 ppm assigned to CH_3 protons. The singlet signals at 6.28 and 6.51 ppm are attributed to the protons of NH_2 groups. These signals are overlapped with the aromatic protons. The aromatic protons appear as multiplet in the region 6.51-7.58 ppm.

The ^{1}H-NMR spectrum of Zr(IV) complex, in DMSO-d_6 shows a broad singlet signal in the downfield region at 10.60 ppm, corresponds to –NH of the amidic group (CO–NH). The presence of this signal confirms the coordination of the ligand in the keto form. The broadening of this singlet signal was attributed to the presence of intramolecular hydrogen bond [23]. The aromatic protons appear as multiplet in the region. 6.68-7.82 ppm.

The ^{1}H-NMR spectrum of Pd(II) complex (Fig. 6), in DMSO-d_6 shows the disappearance of the signal at 10.64 ppm, corresponding to the protons of -NH amidic in the free ligand spectrum. The disappearance of this signal confirms the coordination of the ligand to Pd(II) in the enol form. The two singlet signals assigned to the two NH_2 protons remain in its position as the free ligand, confirming the remaining of these groups inert towards coordination.

Mass spectra

The exact mass of the ligand (2-AAB) appears at m/z = 269.1, which matches with the formula $C_{15}H_{17}N_4O$.

Mass spectrum of Pd(II) complex shows the molecular ion peak at m/z = 463, in agreement with the formula $[Pd(C_{15}H_{16}N_4O)ClH_2O]2H_2O$. The molecular ion loses the three molecules of water successively, leading to the three peaks at *m/z* = 446, 428 and 410, respectively. When the molecular ion loses the fragment $C_6H_4(NH_2)CCH_3$, it gives the peak at *m/z* =317. The peak at *m/z* = 410 is fragmented by loss of Cl giving the base peak at *m/z* = 374, which corresponds to [PdL] species. The base peak loses aniline molecule and gives the ion peak at *m/z* = 237. The fragmentation pattern of $[Pd(C_{15}H_{16}N_4O)ClH_2O]2H_2O$ is indicated in Scheme 1.

The mass spectrum of Zr(IV) complex (Fig. 7) shows the exact mass at *m/z* = 525.2, corresponding to the molecular formula $[Zr(C_{15}H_{17}N_4O)Cl_4]1/2EtOH$. Two possible pathways in the fragmentation pattern of Zr(IV) complex have been suggested. In the first pathway, the molecular ion loses half molecular of ethanol and $ZrCl_4$ giving the base peak at *m/z* = 296, corresponding to the free ligand. The possible fragments of the free organic ligand and Zr(IV) complex are indicated in Scheme 2.

In the second pathway, the molecular ion peak loses amino group and Cl_2 to give the peaks at *m/z* = 509 and 437, respectively. The ion peak at *m/z* = 410 is fragmented by loss of CH_3 and Cl giving the ion peak at *m/z* = 382. The latter peak loses NH_2 and C_2H_2 to give the peak at *m/z* = 346, which further loses methane molecule leading to the peak at m/z = 330. The peak at 330 loses the fragment CH_3C_2 and gives the peak at *m/z* = 291.

Mass spectrum of Ru(III) complex shows the molecular ion peak at m/z = 542 which corresponds to the formula $[Ru(C_7H_{17}N_4O)Cl_3H_2O]2.5H_2O$. Two possible path-ways have been suggested for the fragmentation of Ru(III) complex as indicated Scheme 3. In the first pathway, the molecular ion peak loses three and half molecules of water and three Cl leading to the peak at m/z = 369 corresponding to [RuL]. This peak losses Ru, $C_6H_4(NH_2)C$ and CH_3 to give the base peak at m/z = 161. Another path way could be followed for the fragmentation of [RuL] peak at m/z = 369 by loss of two amino and methyl groups giving the ion peak at *m/z* = 323. The peak at *m/z* = 323 is fragmented to produce the peaks at m/z = 269 and 244 by loss of C_2H_2 and C_4H_4, respectively. The molecular ion peak can follow a second fragmentation pathway by loss of two water molecules and three Cl in five successive steps to give the peaks at *m/z* = 523, 505, 471, 435 and 400 respectively.

Thermal analysis

Thermo-gravimetrical analyses (TGA and DTA) of the complexes were measured from room temperature (25˚C) to 1000˚C. These measurements shed light on the thermal stability of the complexes. Thermo-gravimetrical results are presented in Table 2.

TGA and DTA curves of Ru(III) complex shows that, it loses two and half molecules of hydrated water. This step takes part from 25 to110 ˚C (Exp., 8.9, Calcd. 8.3%), followed by loss of one molecule of water of coordination and 3Cl in an endothermic step from110 to 240 ˚C, (Exp., 21.8, Calcd. 23.0 %) then, methyl group and chloride ion in the range 240-270 ˚C (Exp., 8.0, Calcd. 9.3 %). The organic moiety $C_6H_4CNH_2$ is lost within 270-305 ˚C (Exp. 15.6, Calcd. 16.9%). Finally,

the remaining of the organic ligand ($C_6H_4C_2NH_2NNH$) decomposes in the range 305-570 ˚C (Exp. 24.1, Calcd. 26.7%), leaving Ru_2O_3 as a residue (Exp. 21.6, Calcd. 23.0%)

The thermogrames (TGA and DTA) of Pd(II) complex indicates that, it dissociates from 25 to 120 ˚C by losing the out of coordination sphere water molecules, followed by loss of one coordinated water molecules (120-210 ˚C) (Exp., 4.1, Calcd. 3.9%). The third step is an endothermic one (210-275 ˚C) and corresponds to the loss of Ph and Cl (Exp., 25.1, Calcd. 24.0%). The next step corresponds to loss of the moiety $PhNH_2$ in the range 275-375 ˚C (Exp. 20.9, Calcd. 19.8%). Finally, the remaining of the organic ligand (NH_2, CO, N_2 and CH_3) is lost in the range 375-600 ˚C (Exp. 22.2, Calcd. 21.3 %). The residue is expected to be PdO (Exp. 26.9, Calcd. 26.3 %).

The thermograms of Zr(IV) complex shows that, it loses half molecule of ethanol from 25 to104 ˚C (Exp. 3.9, Calcd. 4.4%). The next step (104-285 ˚C) is an endothermic and corresponds to the loss of $2Cl_2$ and $PhNH_2$ (Exp. 43.3, Calcd. 44.8%). The final step (320-665 ˚C) corresponds to the loss of the remaining organic moiety $PhNH_2CCH_3NNHC$ (Exp. 32.80, Calcd. 33.7%), leaving ZrO_2 as a residue (Exp. 20.0, Calcd. 23.6%)

The thermodynamic parameters of Pd(II), Ru(III) and Zr(IV) complexes were calculated by applying Coats-Redfern [24] procedure and the values are collected in Table 3.

The activation energy E was calculated from the graphical relation (Fig. 8), the enthalpy of activation (ΔH^*), the entropy (ΔS^*) and the free energy of activation (ΔG^*) were calculated using equations 1-3.

$$\Delta S^* = 2.303\ [\log (Zh/KT)]R \quad (1)$$

$$\Delta H^* = E - RT \quad (2)$$

$$\Delta G^* = \Delta H^* - T\,\Delta S^* \quad (3)$$

Where, Z, K and h are the pre-exponential factor, Boltzmann and Plank constants, respectively [25]. The calculations were carried out only on the second step of decomposition where, the activation energies could not be calculated for the overlapping or unsuitable steps.

The relatively high activation energies (E) values indicate the strong bonding between the ligand and the metal ions. The positive enthalpies and free energies indicate that the decomposition processes are endothermic and non-spontaneous, respectively. The complexes have more ordered structure than the decomposition products as indicated from the negative ΔS^* values [26]. From the results it is clear that, Ru(III) complex is the most stable among the tested complexes, then Zr(IV) and finally comes Pd(II) complexes.

Electronic spectra

The electronic spectrum of the ligand in DMSO shows a band in the UV region at 32362 cm^{-1} due to $\pi \rightarrow \pi^*$ transition in the aromatic systems. Another two bands are observed at 28169 and 24570 cm^{-1} attributed to $n \rightarrow \pi^*$ transitions. The later two bands are observed in the spectra of the complexes but shifted to higher frequencies as a result of the coordination of the ligand to the metal ions [27].

The absorption spectrum of Ru(III) complex in DMSO exhibits two bands at 23202 and 16666 cm^{-1} assigned to $^2T_{2g} \rightarrow {}^4T_{1g}$ and $^2T_{2g} \rightarrow {}^4T_{2g}$, $^2A_{1g}$ transitions, respectively. These bands are characteristics of octahedral Ru(III) complexes [28, 29]. The band at 28653 cm^{-1} is attributed to LMCT. Two other bands are observed at 28735 and 32788 cm^{-1} due to the organic ligand transitions.

The spectrum of Pd(II) complex in DMSO shows a band at 21231 cm^{-1} assigned to LMCT. The bands at 28818 and 33003 cm^{-1} are attributed to the ligand transitions.

The electronic spectrum of Zr(IV) complex in DMSO shows a band at 23923 cm^{-1} assigned to LMCT. The two bands at 27932 and 32573 cm^{-1} are attributed to the transitions inside the organic ligand.

X-ray powder diffraction (XRD)

Figure 5 shows the XRD patterns of Pd(II), Ru(III), and Zr(IV) complexes. It is clear that, Pd(II) and Zr(IV) complexes are crystalline while, Ru(III) complex is amorphous. The unit cell parameters of Pd(II) compound was detected by Winplotr software package [30] and showed that

Pd(II) complex crystallizes in monoclinic crystal with the space group $P2_1/c$, a =17.0, b = 8.1, c = 11.8 Å. α = 90, β = 104.77 and γ = 90°. XRD has been treated by the simulated annealing technique in Endeavour 1.7b [31] and the final refinements were carried out by Pawley refinement. Weighted profile R-factor (R_{wp}) value was (8.16) confirmed good agreement between the calculated and the experimental data.

The crystal structure showed three dimensional frameworks are formed through hydrogen bonding and the Pd(II) ions form 1D chains as indicated in Fig. 9. Some geometrical parameters (Table 4) obtained from XRD were compared with that obtained for the optimized structure by PM3 method (Fig. 10). The possibility of interactions and hydrogen bonding between neighboring molecules are not taken in consideration in case of PM3 calculations, it may be the reason for the differences in values between the calculated by PM3 and that determined from XRD.

From the XRD data it is clear that, the C10-O1 bond length (1.410 Å) is larger than the ketonic C=O by 0.18 Å; however it is in the same range as the enolic C-O. This observation confirms the coordination of the ligand to Pd(II) ion in the enol form. The bond lengths of Pd-O1 (1.9755 Å) and Pd-N1 (1.9555 Å) are in the same range as that reported for corresponding crystal structure of similar donors [32]. The Pd-Cl bond length is larger than that reported for similar structure [33], due to the participation of Cl in hydrogen bonding [33]. The angles, N1-Pd-O1 and O1-Pd-O2 are 83.0° and 173.84°, respectively. The deviation from the angles 90 and 180° of the normal square-planar structure may be resulted from the participation of water oxygen in hydrogen bonding and the presence of steric hindrance of the aromatic amino groups of the neighbor molecules.

Morphological characterization

Because of the influence of the particle size and morphology on the properties of materials, the transmittance electron microscope (TEM) images of the isolated complexes were investigated.

Figs. 11A, B and C, shows the TEM images of Ru(III), Pd(II) and Zr(IV) complexes, respectively. It is clear that, the shape of Ru(III) particles are overlapped spheres with average size 442 nm. The particles of Pd(II) complex have rod like shape with length in the range 1.3-11.8 μm

and width 151-371 nm. The particles of Zr(IV) complex are irregular slides with average size 4-25 μm and average width 4 μm, respectively. It is clear that, Ru(III) complex has the smallest particle size and the more regular shape among the three complexes.

Optical band gap

Chromophores containing transition metals have been investigated widely because of their nonlinear optical (NLO) properties [34]. Studying the conductivity properties of metal-organic species gives them potential applicability in molecular electronics, sensors, optoelectronic devices and organic transistors [35, 36].

In this study the optical band gaps of Pd(II), Ru(III) and Zr(IV) complexes were determined from the electronic absorption spectrum of these complex in DMSO. The absorption coefficient (α) was calculated from the measured absorbance (A) by applying the relation $\alpha = 1/d \ln A$ (1) where, d is the width of the cell. The optical band gap energy (E_g) is calculated from the relation: $\alpha h\nu = A (h\nu - E_g)^m$ (2), where m equal to 2 and 1/2 for direct and indirect transitions, respectively, A is an energy independent constant [37, 38]. By plotting $(\alpha h\nu)^2$ vs. hν and by extrapolating the linear part of the curve to $(\alpha h\nu)^2 = 0$, the direct band gap was determined. The curves (Fig. 12) indicate the band gap values (E_g) are 3.15, 3.22 and 3.31 eV for Pd(II), Ru(III) and Zr(IV) complexes, respectively. These values suggest that these complexes are semi-conductors. Comparing the values of (E_g) with that of highly efficient photovoltaic materials clarifies that the present complexes are potential compounds for harvesting solar radiation in solar cell devices [39].

Anti-inflammatory and analgesic activities of (2-AAB) and its complexes

An *in-vivo* pharmacological evaluation of the ligand (2-AAB) and its Ru(III), Pd(II) and Zr(IV) complexes was carried out to asses their potential anti-inflammatory and analgesic activities. The results of this study (Table 3) showed that, the animals treated by meloxicam, (2-AAB), and Ru(III) complex reduces the inflammation comparing with the arthritic non-treated group. These compounds recorded a significant activity in lessening the rheumatoid index (RI) against the

arthritic non-treated group, while Pd(II) and Zr(IV) complexes produced non-significant change of the rheumatoid index (RI) against the arthritic non-treated group.

The analgesic effect increases in groups of animals treated with Pd(II), Zr(IV) and Ru(III) complexes as compared with that of the arthritic non-treated group. It is worthnoting that Ru(III) complex treated group has a better analgesic effect than meloxicam. On the other hand, the ligand (2-AAB), Pd(II) and Zr(IV) complexes produced non-significant change of pain tolerance compared with that of the arthritic non-treated group.

The highest anti-rheumatic activity of Ru(III) complex compared with the other investigated compounds could be attributed to its regular spherical shape and smallest particles size which is expected to facilitate its transportation through the cell membrane.

Conclusion

Literature survey showed no work and no pharmacological assay have been carried out on *(E)*-2-amino-N-(1-(2-aminophenyl)ethylidene)benzohydrazide (2-AAB) and its Pd(II), Ru(III) and Zr(IV) complexes. The ligand (2-AAB) can coordinate to the investigated metal ions either in the keto or in the enol form. Optical band gap measurements showed that the isolated complexes are semi-conductors and can be used as harvesting material in solar cell devices.

The anti-inflammatory activity showed that, Ru(III)complex has the highest anti-inflammatory activity among the tested compounds. New complexes of the second and / or the third transition series with hydrazone moiety are expected to be potent anti-rheumatic agents.

Acknowledgment

The author Dr. Nasser M. Hosny acknowledges Prof. Jorge A. Navarro, Inorganic Chemistry Department, Granada University and the Centro de Instrumentacion Cientifica, Granada University, Spain for carrying out some of the analyses.

References

[1] H. Khanmohammadi, M. Erfantalab, G. Azimi, Spectrochimica Acta A, 105 (2013) 338.

[2] A.Taha, A. A. Emara, M. M. Mashaly, O.M.I. Adly, Spectrochimica Acta A, 130(2014) 429.

[3] I. Kaya, S. C. ulhao glu, M. Gul, Synthetic Met., 156 (2006)1123.

[4] P. Cerrada, L. Oriol, M. Pinol, J. L. Serrano, J. Am. Chem. Soc., 119 (1997) 7581.

[5] K. Andjelkovic, M. Sumar, I. Ivanovic-Burmazovic, Therm. Anal. Calorm., 66 (2001) 759.

[6] C. Hoose, K. Eberhardt, W. Hartmann, W. Wosniok, Pneumologie, 44(10)(1990) 459.

[7] V. N. Saliaev, N. S. Titov, V. P. Ermlaev, Farmakol Toksikol, 43(4)(1980) 372.

[8] H. Vidrio, G. Fernandez, M. Medina, E. Al varez, F. Orallo, Vasc. Pharmacol., 40(1) (2003) 13.

[9] E. M. Becker, D.B. Lovejoy, J. M. Greer, R. Watts, D. R. Richardson, Brit. J. Pharmacol. 138 (2003) 819.

[10] P. Lipsy, Am. J. Med., 110 (2001) 1S.

[11] A. Palomer, F. Cabre, J. Pascual, J. Campos, M. Trujillio, A. Entrena, M. Gallo, L. Garcia, D. Maulcon, A. Espinosa, J. Med. Chem. 45 (2002) 1402.

[12] J. J. Talley, D. L. Brown, J. S. Carter, M. J. Graneto, C. M. Koboklt, J. L. Masferrer, W. E. Perkins, R. S. Rogers, A. F. Shaffer, A. F. Zhang, Y. Y. Zweifel, B. S. Seibert, J. Med. Chem., 43 (2000)775.

[13] A. I. Vogel, "A Text Book of Quantitative Inorganic Analyses", 2nd Ed., Longman, London, 1961.

[14] D. E. Trentham, A. S. Townes, and A. H. Kang, J. Exp Med., 146 (1977)857.

[15] R. Halmdahal, V. Malmstrom E. Vuorio, Ann. Med., 25 (1993) 251.

[16] Paget and Barnes, Evaluation of Drug Activities. In, Laurence and Bacharach. (eds). Pharmacometrics, New York: Academic Press; 1964.

[17] W. J. Geary, Coord. Chem. Revs., 7 (1971) 81.

[18] N. M. Hosny, A.M. Shalaby, Transition Met. Chem., 32**,** (2007) 1085.

[19] N. Nawar, N. M. Hosny, Chem. Pharm. Bull., 47 (1999) 944.

[20] N. M. Hosny, J. Mol. Struct., 923 (2009) 98.

[21] K. Nakamoto, "Infrared Spectra of Inorganic and Coordination Compounds", John Wiley, NewYork, 1970.

[22] Misbah ur Rehman, M. Imran, M Arif, Am J Appl Chem, 1(2013)59-66.

[23] A. Maiti, S. Ghosh, Inorg. Biochem., 36 (1989) 131.

[24] A.W. Coats, J.P. Redfern, Nature 201 (1964) 68-69.

[25] Y. E. Sherif, N. M. Hosny, Eur J Med Chem 83(2014)338-343.

[26] N. M. Hosny, M. A. Hussien, F. Radwan, N. Nawar, Spectrochim Acta A, 132(2014)121-129.

[27] A. Reiss, M. Mureseanu, J. Chil. Chem. Soc, 57 (2012) 1409-1414

[28] M. M. T. Khan, D. Srinivas, R. I. Kureshy, N. H. Khan, Inorg. Chem., 29 (1990) 2320.

[29] V. K. Sharma, A. Srivastava S. Srivastava, J. Serb. Chem. Soc. 71 (8–9) (2006) 917.

[30] H. Putz, J.C. Schon, M. Jansen, J. Appl. Cryst., 32(1999) 864

[31] Crystal Impact GbR, Endeavour 1.7, Internet: http://www.crystalimpact.com/endeavour.

[32] M. Sik Y. R. Ramesh, J. Kim, D. Ryu, K. H. Ahn, J. Organomet. Chem., 691(2006)5927.

[33] W. Liufang, P. Zhouren, W. Xin, Polyhedron, 12(1993)1505.

[34] B. J. Coe, Coord .Chem. Rev., 257(2013)1438.

[35] F. Karipcin, B. Dede, Y. Caglar, D. Hur, S. Ilican, M. Caglar, Y. Sahin, Opt. Comm**,** 272 (2007) 131.

[36] F. Yakuphanoglu, A.Cukurovali, I. Yilmaz, Opt. Mater., 27 (2005)1363.

[37] J. Tauc, R. Grigorovici, A. Vancu, Phys. Status Solid, 15(1966)627.

[38] R. K. Pandey, S.N. Sahu, S. Chandra, "Handbook of Semiconductor Electrodeposition", Marcel Dekker, Inc., New York, 1996, p. 142.

[39] M. L. Fu, G. C. Guo, X. Liu, L. Z. Cai, J. S. Huang, Inorg. Chem. Comm., 8(2005) 18.

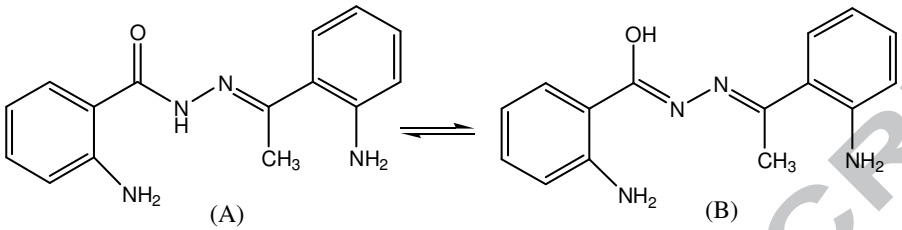

Fig. 1. (A) Keto, (B) enol tautomeric forms of the ligand

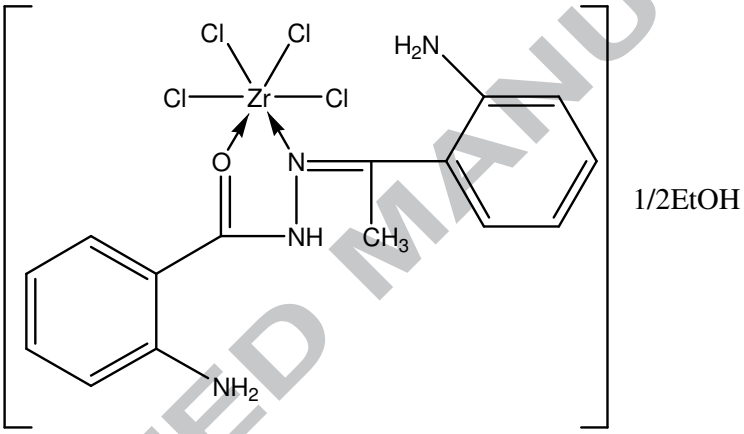

Fig. 2. Suggested structure of Zr(IV) complex

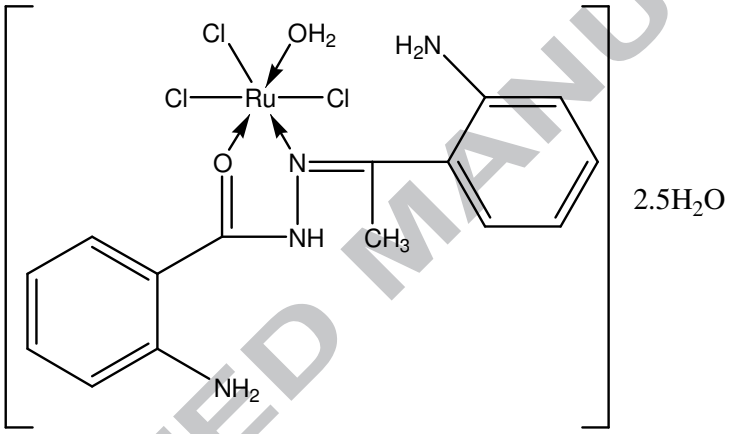

Fig. 3. Suggested structure of Ru(III) complex

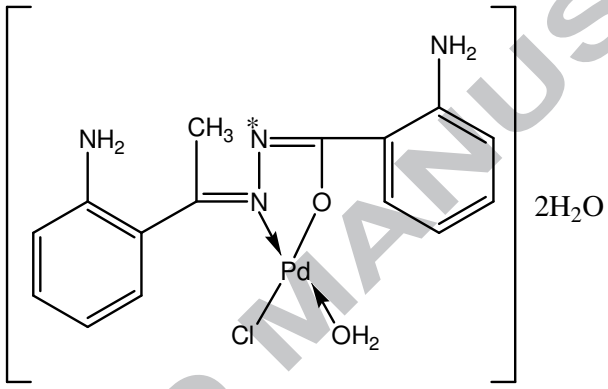

Fig. 4. Suggested structure of Pd(II) complex

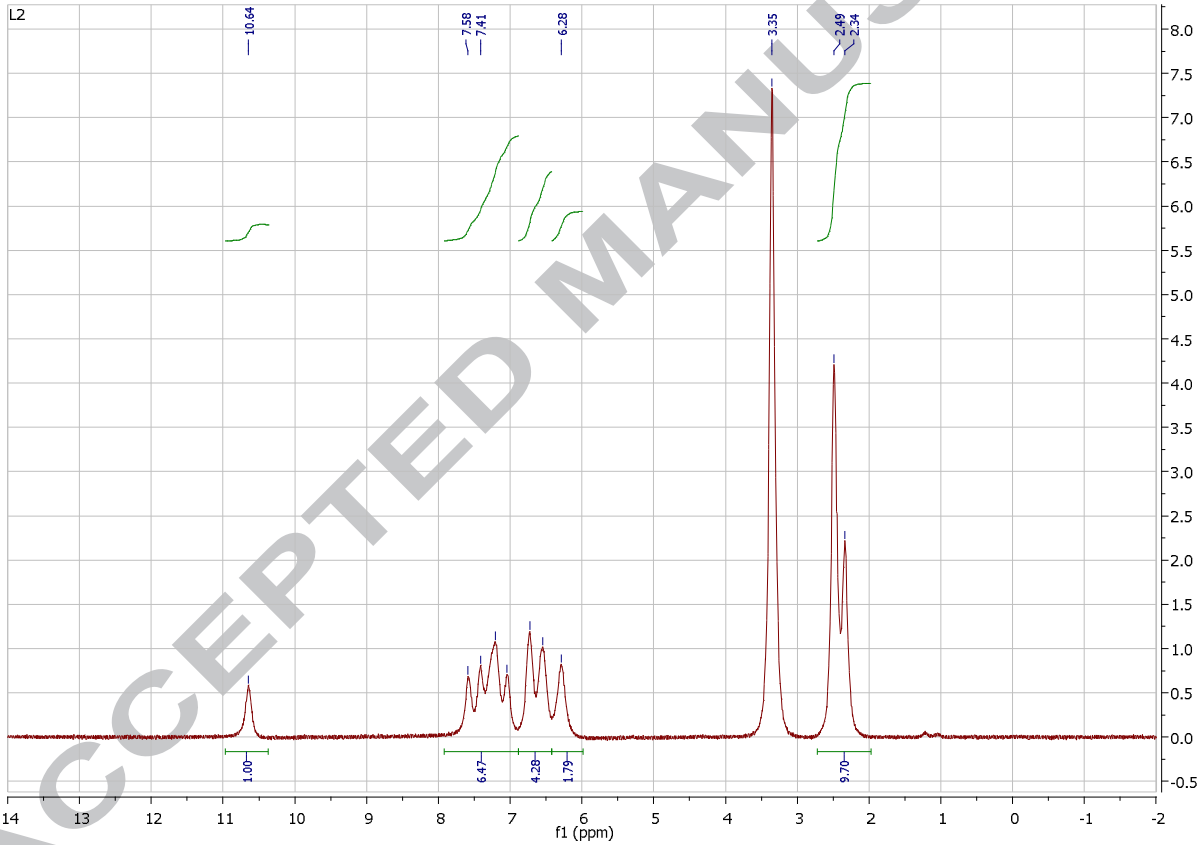

Fig.5. ^{1}H-NMR spectrum of the ligand

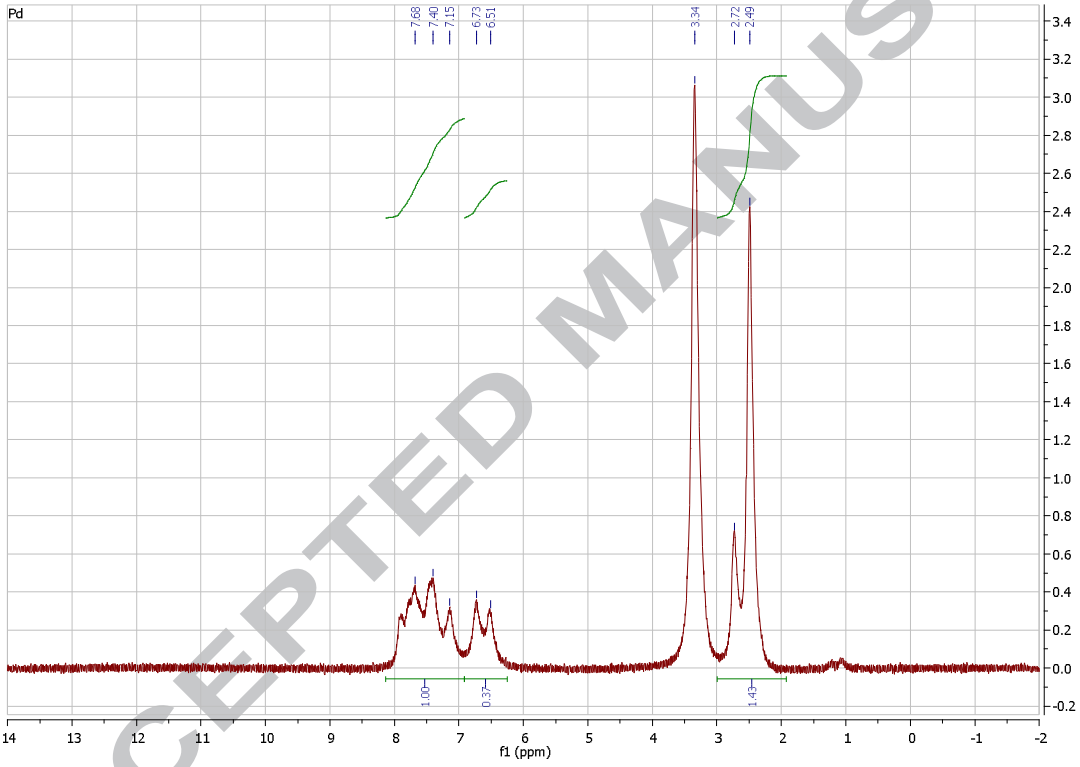

Fig.6. ^{1}H-NMR spectrum of Pd(II) complex

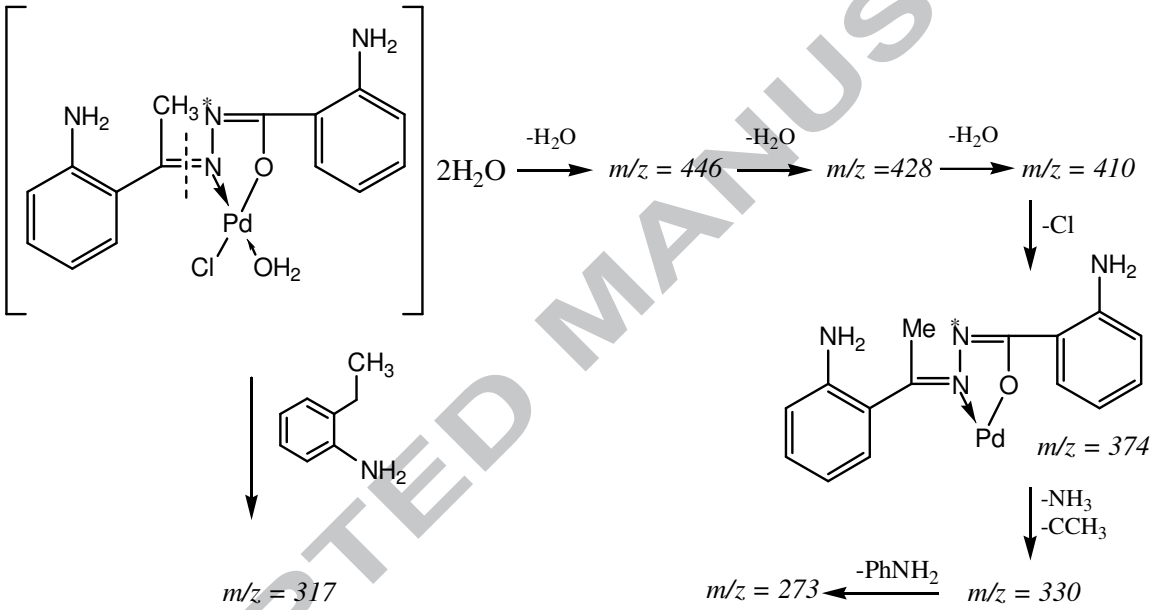

Scheme 1. Fragmentation pattern of Pd (II) complex

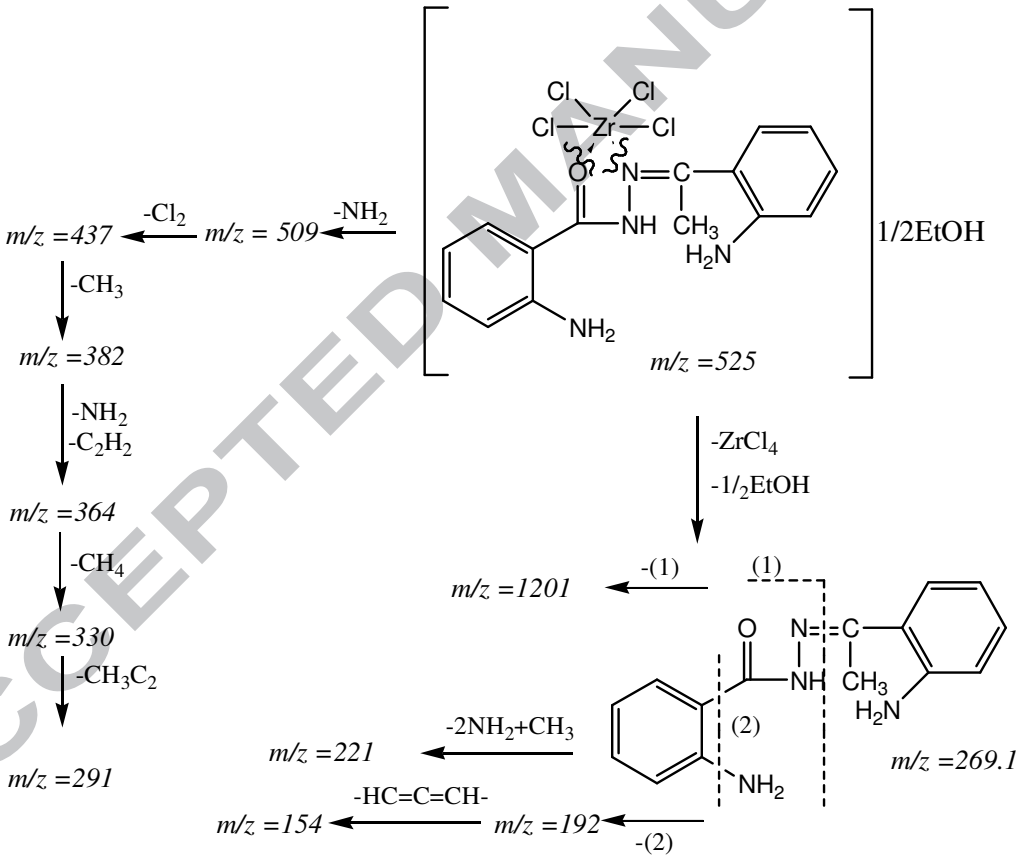

Scheme 2. Fragmentation pattern of Zr(IV) complex

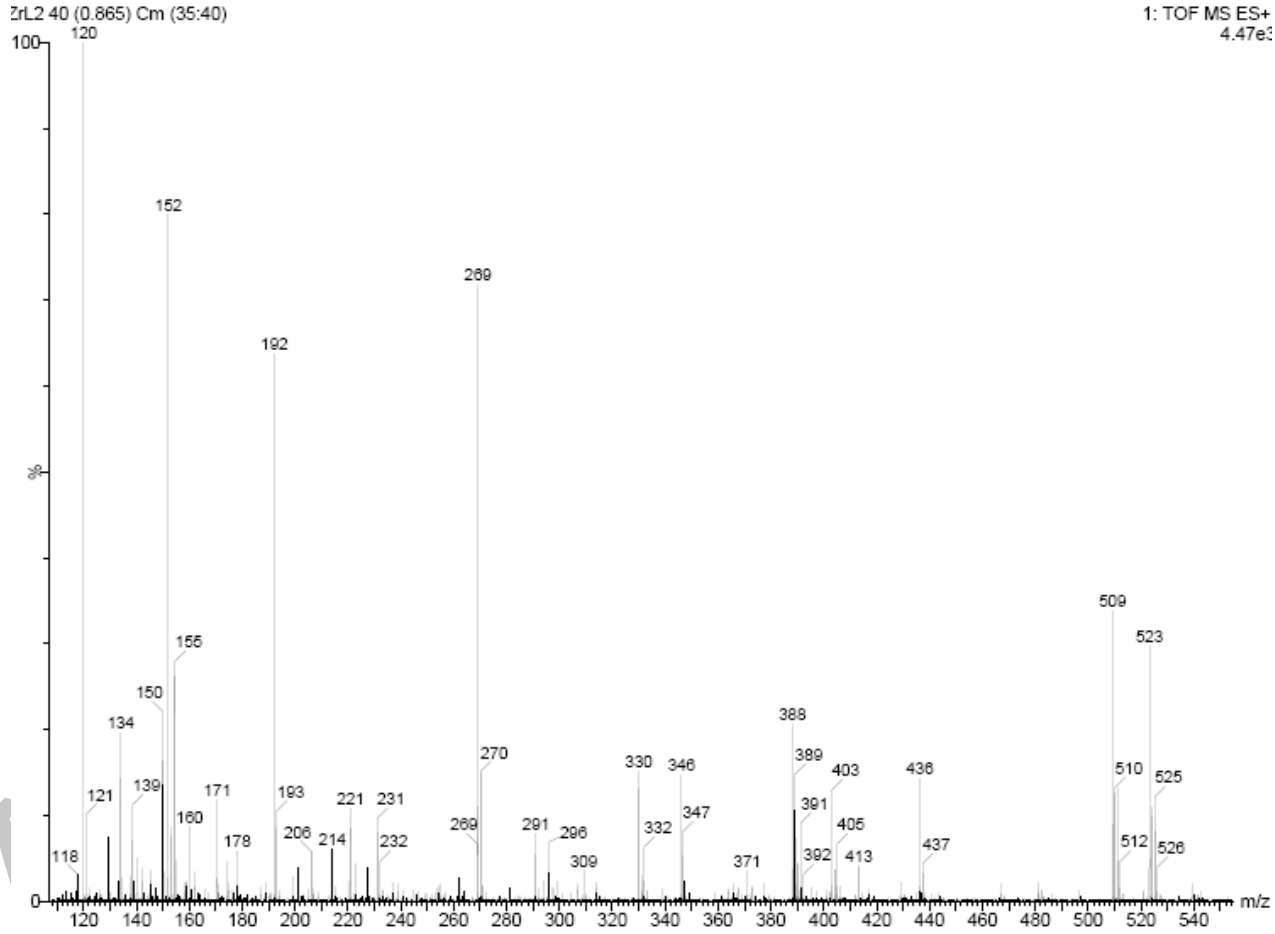

Fig.7. ES-MS of Zr(IV) complex

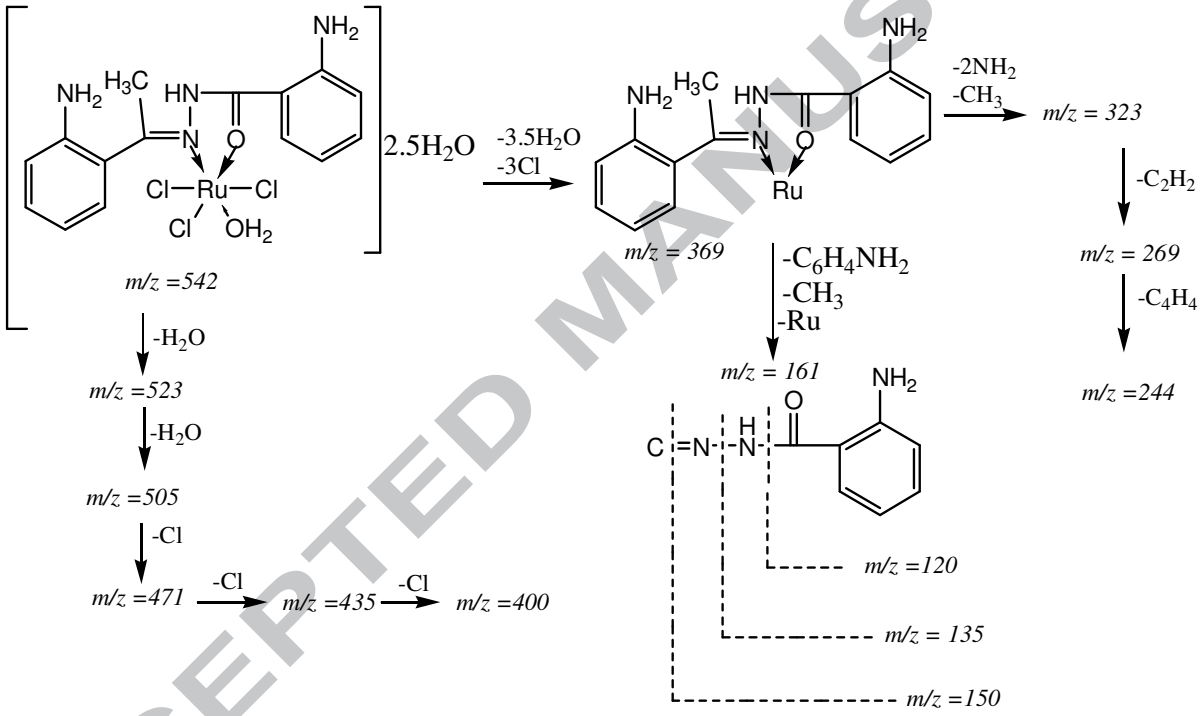

Scheme 3. Fragmentation pattern of Ru (III) complex

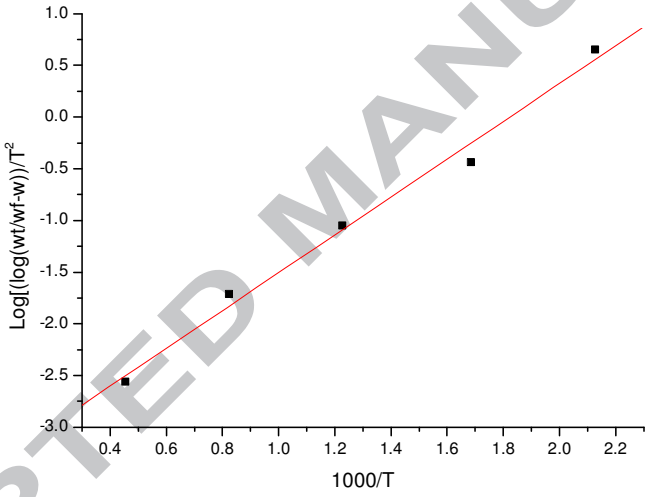

Fig. 8. Coats-Redfern plot for the second stage of the thermal decomposition of Pd(II) complex

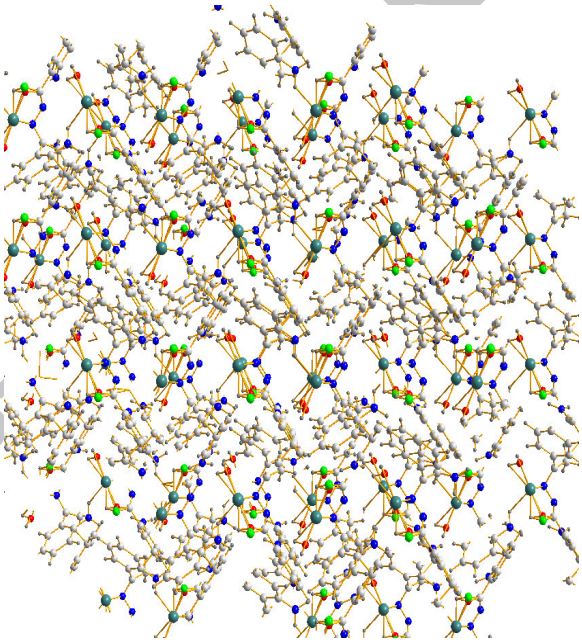

Fig.9. Crystal packing viewed along c axis, indicating 1D chains of Pd (II) in dark green color

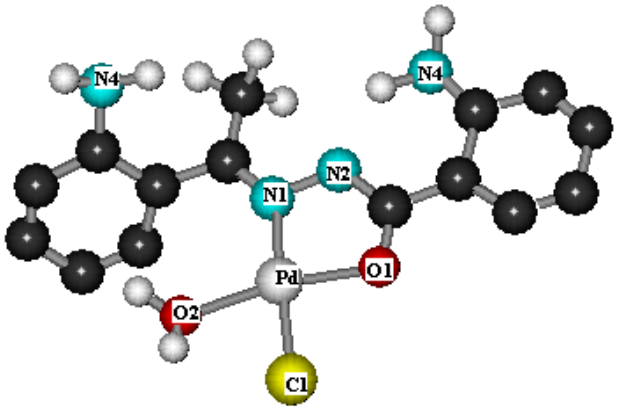

Fig.10. Representation of the molecular structure of Pd(II) complex

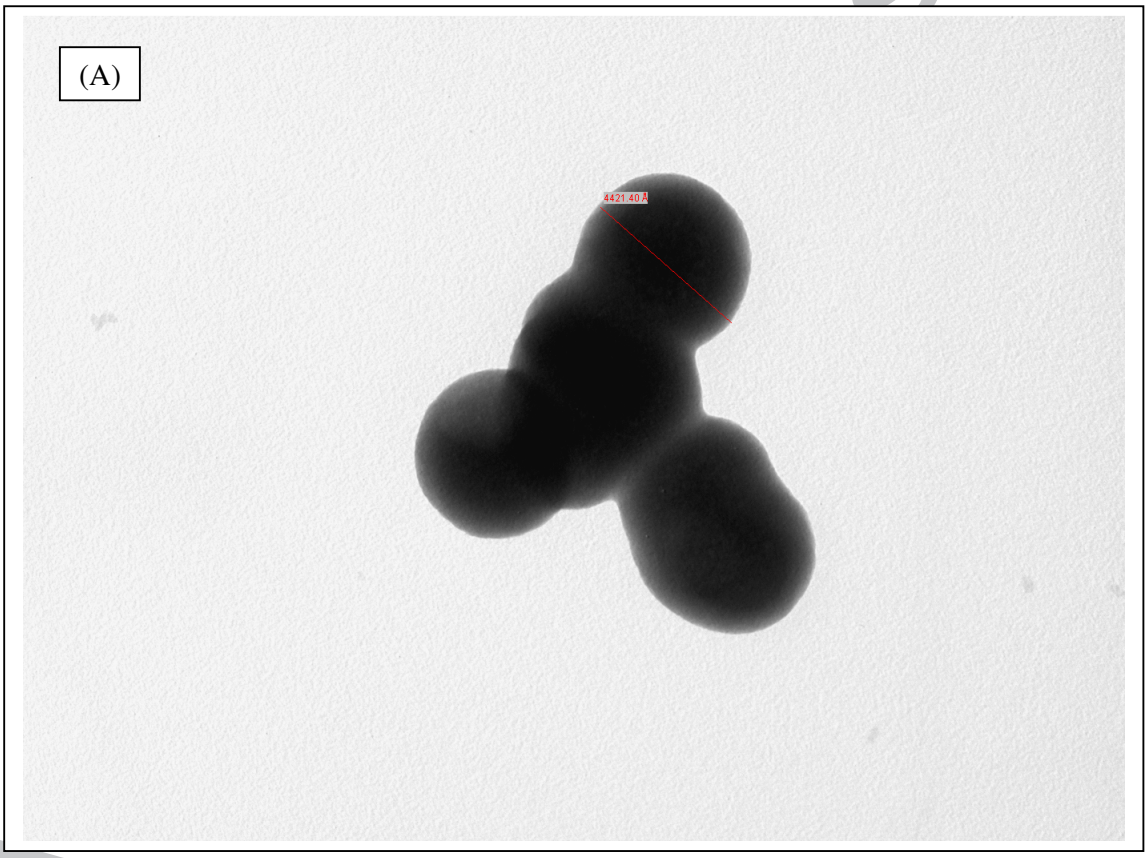

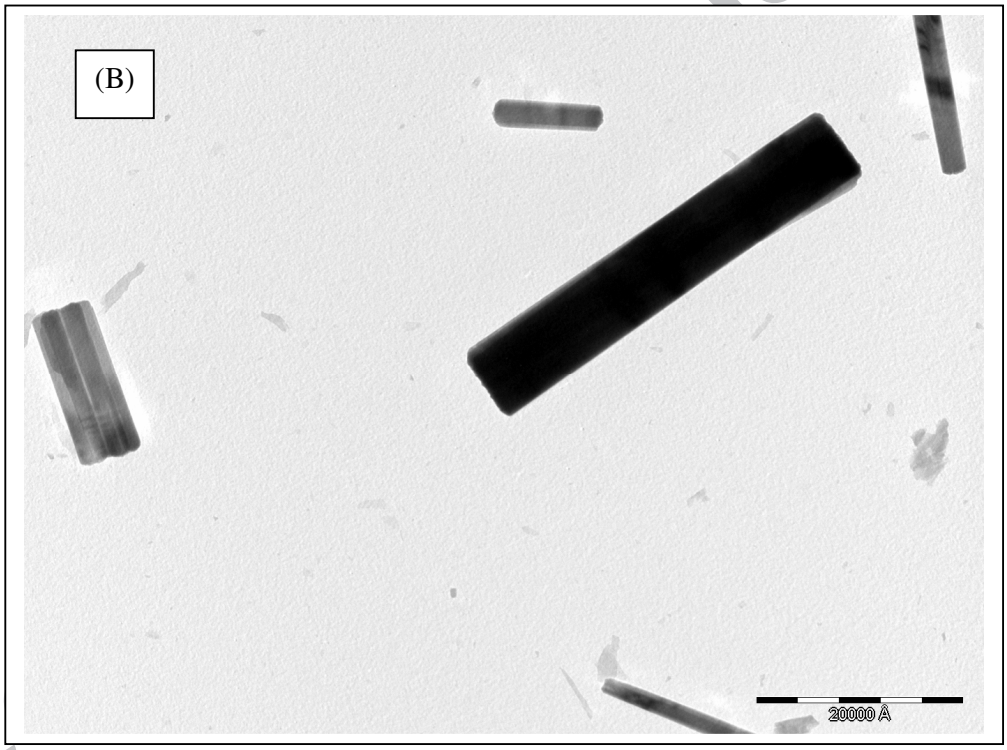

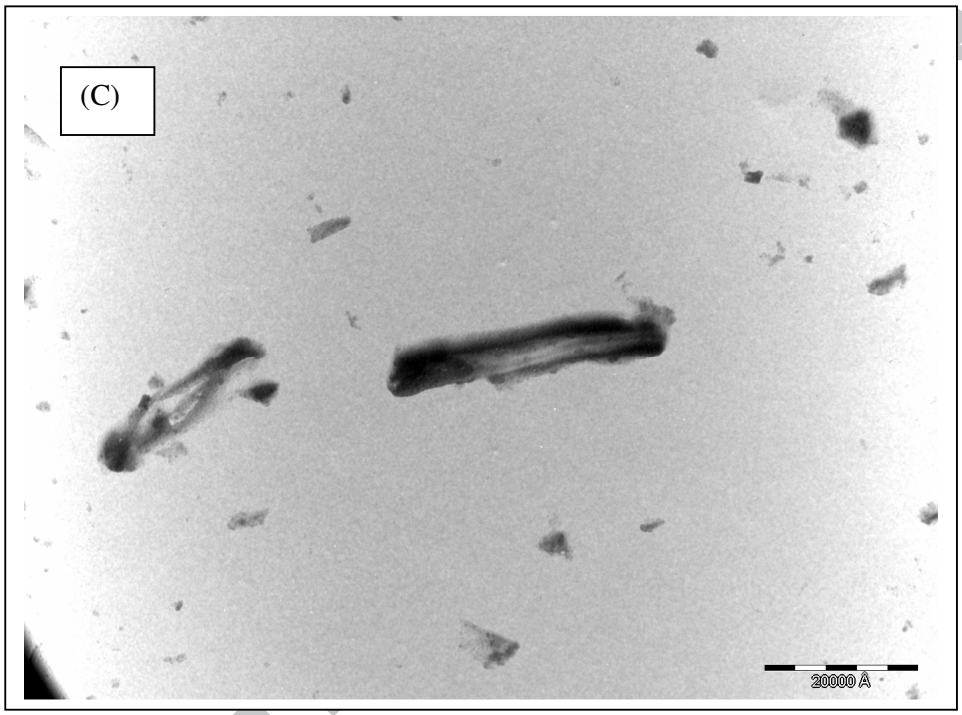

Fig.11. TEM of (A) Ru(III) complex, (B) Pd(II) complex and (C) Zr (IV) complex.

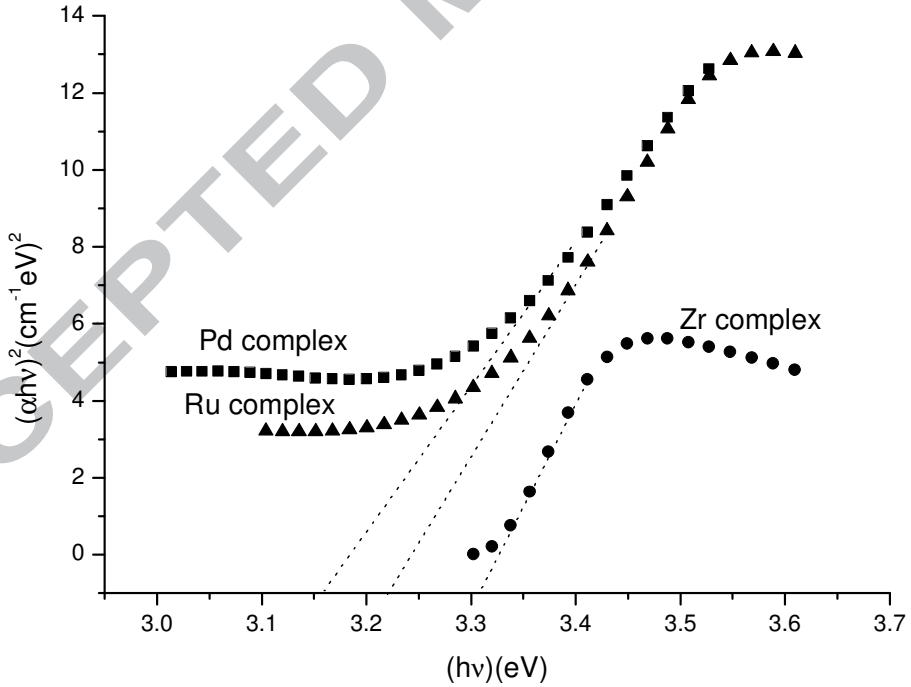

Fig. 12. Optical band gap of Pd(II), Ru(III) and Zr(IV) complexes

Table1
IR spectral data of Pd(II), Ru(III) and Zr(IV) complexes.

Compound	$\nu(NH_2)$	ν(C=N)	ν(C=O)	ν(CONH)	$\delta(NH_2)$	ν (N-N)	ν(M-O)	ν(M-N)
(2-AAB)	3480, 3458, 3366, 3215	1600	1631	1574	1612	970	-	-
[Pd(2-AAB)Cl H_2O]2H_2O	3398,3310	1608, 1590	-	-	1601	985	533	489
[Ru(2-AAB)3Cl.H_2O]2.5H_2O	3440, 3213	1610	1645	1567	1589	991	570	440
[Zr(2-AAB)Cl_4]0.5EtOH	3423, 3404	1624	1666	1560	1595	994	551	483

Table 2.
Thermo-gravimetrical results (TG) of Pd(II), Ru(III) and Zr(IV) complexes.

Complex	T range (◦C)	Mass loss Estim (Calcd%)	Assignment
[Ru(2-AAB)3Cl.H_2O]2.5H_2O	25-110	8.9(8.3)	Loss of 2.5 H_2O (hydrated)
	110-240	21.8(23.0)	Loss of H_2O (coordinated)+ 3Cl
	240-270	8.0(9.3)	Loss of CH_3 and Cl
	270-305	15.6(16.9)	Loss of $C_6H_4CNH_2$
	305-570	24.1(26.7)	Loss of $C_6H_4C_2NH_2NNH$
	570-1000	21.6(23.0)	Residue Ru_2O_3
[Pd(2-AAB)Cl H_2O]2H_2O	120-210	4.1(3.9)	Loss of H_2O (coordinated)
	210-275	25.1(24.1)	Loss Ph and Cl
	275-375	20.9(19.8)	Loss of $PhNH_2$
	375-600	22.2(21.3)	Loss of NH_2, CO, N_2 and CH_3
	600-1000	26.9(26.3)	Residue of PdO
[Zr(2-AAB)Cl_4]0.5EtOH	25-104	3.9(4.4)	Loss of 0.5EtOH
	104-285	43.3(44.8)	Loss of 2Cl_2 and $PhNH_2$
	320-665	32.8(33.7)	Loss of $PhNH_2CCH_3NNHC$
	665-1000	20.0(23.6)	Residue ZrO_2

Table 3.
Thermodynamic parameters of Pd(II), Ru(III) and Zr(IV) complexes

Compound	Decomposition range ºC	E (KJ.mol^{-1})	-Δ S (J.K. mol^{-1})	ΔH (KJ.mol^{-1})	Δ G (KJ.mol^{-1})
[Pd(2-AAB)Cl H_2O]2H_2O	180-210	424	110.6	419.7	473.8
[Ru(2-AAB)3Cl.H_2O]2.5H_2O	110-240	600.2	103.0	596.0	646
[Zr(2-AAB)Cl_4]0.5EtOH	104-285	953.7	100.4	949	1002.3

Table 4.
Selected bond lengths [Å] and angles [°] for Pd(II) complex

bond	XRPD	PM3
C5- C10	1.5398	1.4671
C7- C8	1.3235	1.3959
C8- C9	1.6014	1.4927
C9- C11	1.3246	1.3559
C10- N4	1.2441	1.3334
C10- O1	1.4103	1.2894
C10- N1	1.4466	1.40867
C11-C12	1.5390	1.4087
C12-C13	1.3859	1.4037
C13-C15	1.3864	1.3559
C13-C7	1.5400	1.4498
C14-C15	1.5397	1.4531
N1-C15	1.4466	1.3788
N1-N4	1.3517	1.3977
N2-C7	1.4459	1.3788
N3-C6	1.4456	1.4087
Pd1-O2	1.9194	1.985
Pd1-O1	1.9755	2.068
Pd1-N1	1.9555	1.9395
Pd1-Cl1	2.2699	2.3183
O1- Pd -O2	173.84	168.72
N1-Pd- O1	83.83	87.01
O1-Pd-Cl1	90.03	90.36

Table 5.

Influence of meloxicam, the ligand and its Pd(II), Ru(III) and Zr(IV) complexes on rheumatoid factor, pain tolerance, and mobilization tolerance in adjuvant induced rheumatoid arthritis model in rats (M ± S.E), n, number of rats = 6

Group	Dose (mg/ 200 g of rat weight)	Morphology (Inflammation)	Edema	Analgesic effect	
				Pain tolerance	Pain scoring
Non Art Non Treat	[SCMC]solvent	1±0	2.33±0.21	14.33±2.01	1±0
Arth Non Treat	[SCMC]solvent	3.67±0.21*	5.0±0.37*	1.33±0.21*	3.67±0.21*
molexicam	0.38mg	2.67±0.21©	4.3±0.42*	3.33±0.84*	2.67±0.21*
(2-AAB)	0.29	2.67±0.21©	5.5±0.66*	4.0±0.63*	3.67±0.21*
Pd complex	0.65	3.33±0.21*	5.83±0.11*	4.33±0.56*	3.33±0.21*
Zr complex	0.56	3.33±0.21*	5.0±0.36*	6.67±1.11*©	3.33±0.42*
Ru complex	0.65	2.33±0.21©€∞	4.20±0.27*€	9.33±2.1*©®€	3.0±0.37*

Compare with group NonArth Non treated
©Compare with group Arth Non treated
®Compare with molexicam
€ Compare with pd complex

Graphical Abstract

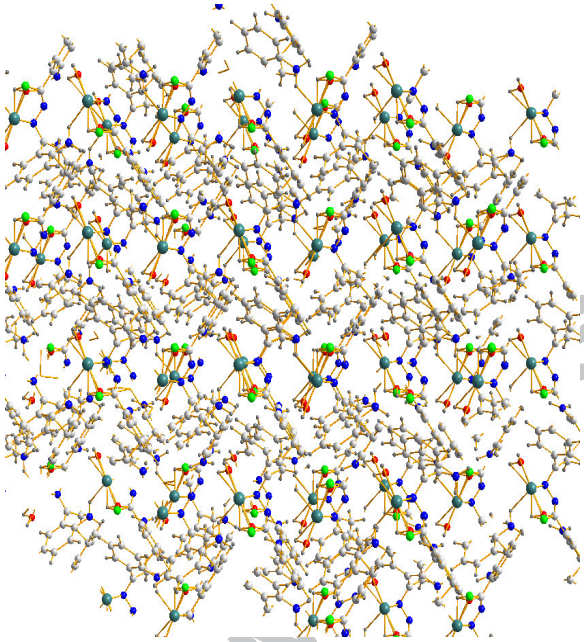

Crystal packing along c axis, highlighting the 1-D chains of palladium ions

Research highlights

- The ligand exists either in the keto or in the enol form
- The ligand coordinates to the metal ions in a bi-dentate manner
- *In-vivo* pharmacological evaluation indicated that Ru(III) has higher activity than the tested compounds.